STOCHASTIC STATISTICAL THEORY OF PRECIPITATION IN METASTABLE ALLOYS WITH APPLICATION TO Fe-Cu AND Fe-Cu-Mn ALLOY SYSTEMS

K. Yu. Khromov[a], F. Soisson[b], A. Yu. Stroev[a] and V. G. Vaks[a]

[a] Russian Research Centre "Kurchatov Institute", Moscow, Russia
[b] Service de Recherches de Metallurgie Physique, CEA, Saclay, France

Schematic phase diagram of a phase separating alloy

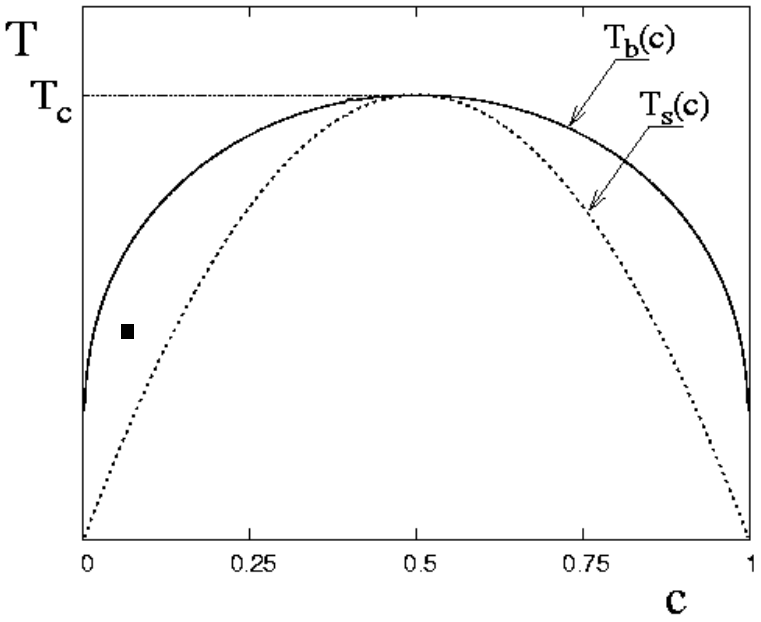

Reduced supersaturation

$$s(c,T) = [c - c_b(T)]/[c_s - c_b(T)]$$

$c_b(T)$ **and** $c_s(T)$ **are concentrations at the binodal and the spinodal at the given temperature T**

Theoretical approaches to simulations of precipitation kinetics

- **Kinetic Monte Carlo approach (KMCA): The most reliable but time consuming, lattice misfit effects cannot be easily taken into account**

- **Phase field method: is widely used, but continuous approximation and mean field or CALPHAD thermodynamic potentials may lead to errors, while treatment of fluctuative terms appears to be arbitrary.**

- **Stochastic statistical approach (SSA): consistent and computationally efficient**

Classical theory of nucleation

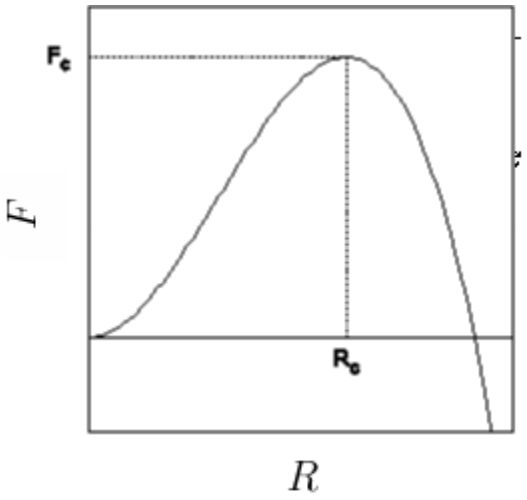

1. Classical theory of nucleation (CTN).

$$F = 4\pi\sigma R^2 - \Delta f \frac{4}{3}\pi\sigma R^3; \qquad \frac{\partial F}{\partial R} = 0, \qquad R_c = \frac{2\sigma}{\Delta f}, \qquad F_c \sim \frac{\sigma^3}{\Delta f^2}.$$

Probability of critical fluctuation:

$$W \sim \exp(-F_c/T) \sim \exp(-\sigma^3/T\Delta f^2).$$

2. Generalizations of CTN. Cahn and Hilliard (1959) used the Ginzburg-Landau-type free energy functional to allow for non-uniformity of a critical embryo. However, their approach is valid only at high $T \sim T_c$ and for large embryos when the discrete lattice effects are small. Dobretsov and Vaks (1998) generalized this approach to take into account the discrete lattice effects, which will be referred to as the "classical theory of nucleation for discrete lattice" (CTN-DL), and below we show some results of this approach.

However, all these purely thermodynamic treatments disregard the fluctuative nature of the nucleation process. Therefore, even though these approaches are useful to understand the general trends in dependences of nucleation kinetics on thermodynamic parameters, their results are shown below to have typically little in common with properties of real new-formed precipitates.

Some experimental data on precipitation of copper in Fe-Cu–based steels

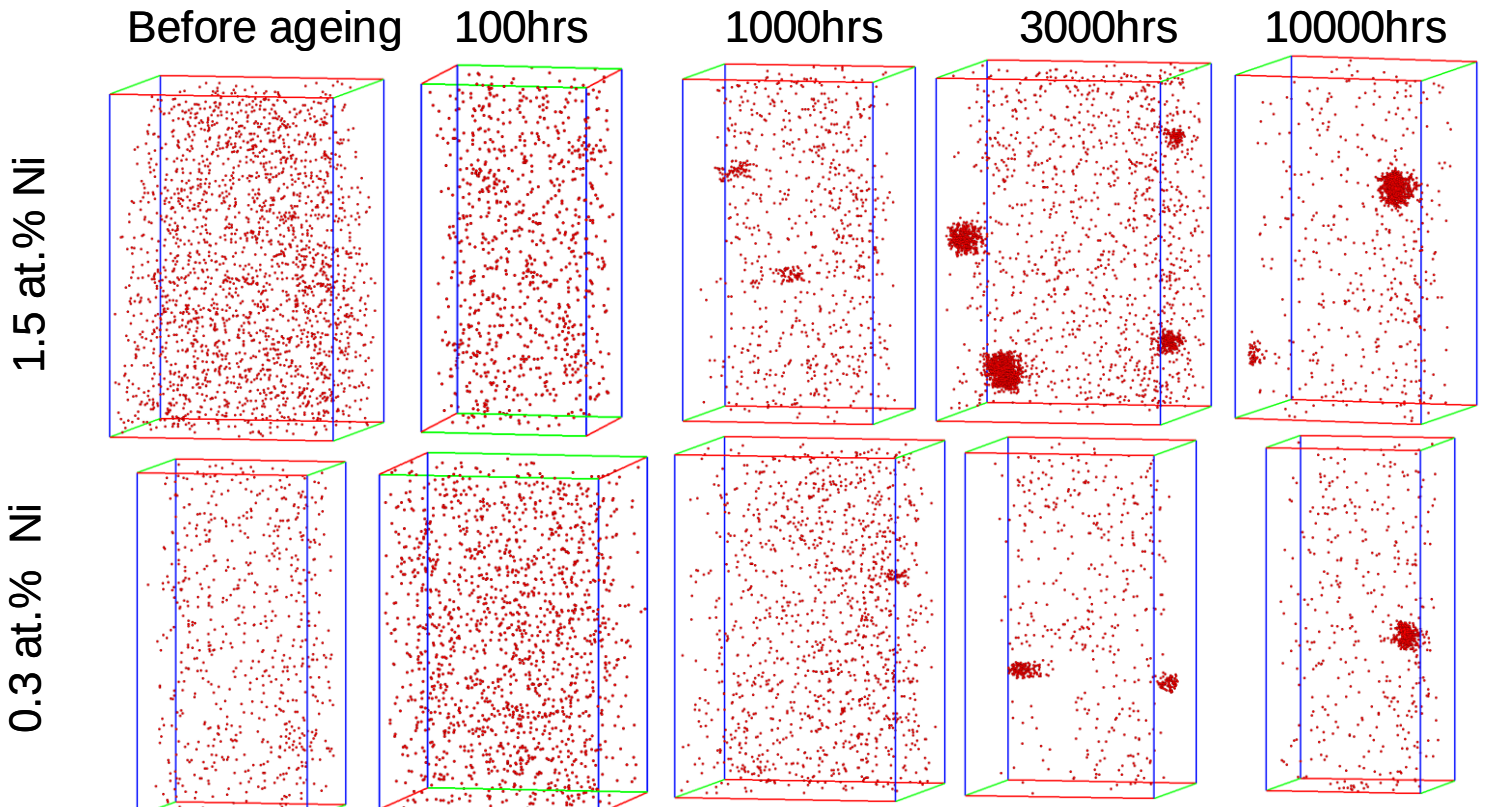

Atomic probe tomography (APT) data by Cerezo et al. (2005). Concentration of Cu, Mn and Si is 0.5, 1.5 and 0.75 at.%, respectively.

Some experimental data on precipitation of copper in Fe-Cu–based steels

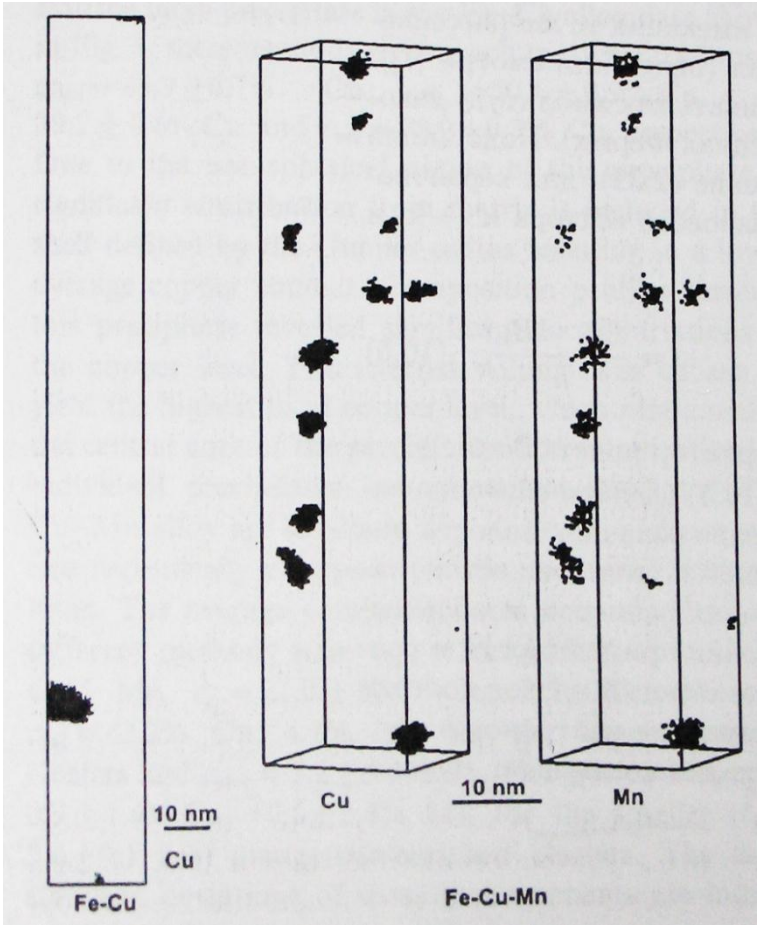

APT data for neutron-irradiated alloys by Miller et al. (2003).

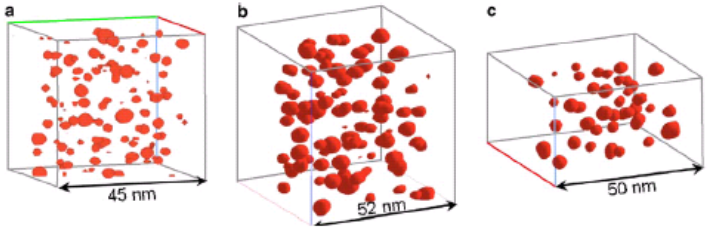

Copper-rich precipitates in the NUCu-150 steel with an isoconcentration surface at a 5 at.% copper threshold level after aging at 773 K for (a) 2 h, (b) 24 h, or (c) 100 h.

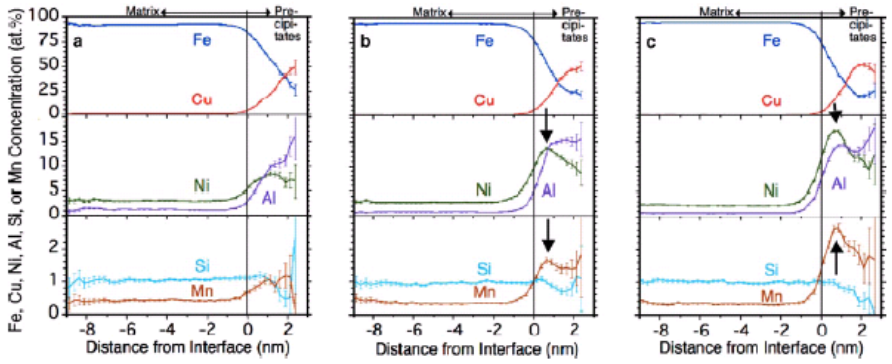

Concentration profiles for copper-rich precipitates in the NUCu-150 steel after the same treatments as in the upper figure (Isheim et al., 2006)

Generalized Gibbs distribution approach (GGDA)

We consider a substitution alloy A-B with vacancies v (ABv alloy). Its configurations are described by the occupation number sets $\{n_{\mathrm{p}i}\}$ where p is A, B or v; $n_{\mathrm{p}i}$ is 1 when site i is occupied by an atom p and zero otherwise; $n_{\mathrm{A}i} + n_{\mathrm{B}i} + n_{\mathrm{v}i} \equiv 1$. Our approach is based on the general master equation for the probability P to find the number set $\{\mathrm{p}i\} = \xi$:

$$dP(\xi)/dt = \sum_{\eta} [W(\xi, \eta) P(\eta) - W(\eta, \xi) P(\xi)], \tag{1}$$

where $W(\xi, \eta)$ is the $\eta \to \xi$ transition probability per unit time. Adopting the "thermally activated atomic exchange model", we can write W as a sum of probabilities W_{ij}^{pq} of elementary inter-site exchanges ("jumps") $\mathrm{q}j \leftrightarrow \mathrm{p}i$:

$$W_{ij}^{\mathrm{pq}} = n_{\mathrm{p}i} n_{\mathrm{q}j} \omega_{ij}^{\mathrm{pq}} \exp[-\beta(E_{\mathrm{p}i,\mathrm{v}j}^{SP} - \hat{E}_{\mathrm{p}i,\mathrm{v}j}^{in})] \equiv n_{\mathrm{p}i} n_{\mathrm{q}j} \gamma_{ij}^{\mathrm{pq}} \exp(\beta \hat{E}_{\mathrm{p}i,\mathrm{q}j}^{in}); \quad \gamma_{ij}^{\mathrm{pq}} = \omega_{ij}^{\mathrm{pq}} \exp(-\beta E_{\mathrm{p}i,\mathrm{v}j}^{SP}). \tag{2}$$

Here $\omega_{ij}^{\mathrm{pq}}$ is the attempt frequency, $\beta = 1/T$ is the reciprocal temperature, $E_{\mathrm{p}i,\mathrm{q}j}^{s}$ is the saddle point energy, and $\hat{E}_{\mathrm{p}i,\mathrm{q}j}^{in}$ is the initial (before the jump) configurational energy.

For the usual conditions of phase transformations, the probability P in (1) can be shown to have the form of the generalized Gibbs distribution (GGD):

$$P\{n_{\mathrm{p}i}\} = \exp\ [\beta\,(\Omega + \sum_{\mathrm{p}i} \lambda_{\mathrm{p}i} n_{\mathrm{p}i} - \sum_{\mathrm{pq},i>j} V_{ij}^{\mathrm{pq}} n_{\mathrm{p}i} n_{\mathrm{q}j})]. \tag{3}$$

Here λ_i (being, generally, both time- and space-dependent) can be called "site chemical potentials"; the last term describes configurational interactions supposed to be pairwise; and Ω is determined by normalization.

Quasi-equilibrium kinetic equation

For simplicity, first we consider the direct atomic exchange (DAE) models; their equivalence to more realistic, vacancy-mediated exchange (VME) models is discussed below. Multiplying master equation (1) by the operator $n_{Ai} \equiv n_i$ and summing over *all* configurational states (which implies neglecting fluctuations of atomic fluxes discussed below), we obtain the "quasi-equilibrium" kinetic equation (QKE):

$$dc_i/dt = \sum_j M_{ij}\, 2\sinh[\beta(\lambda_j - \lambda_i)/2]. \tag{4}$$

Here mean occupations of sites ("local concentrations") c_i correspond to averaging n_i over the GGD (3):

$$c_i = \langle n_i \rangle = \sum_{\{n_j\}} n_i\, P\{n_j\}, \tag{5}$$

while dependences of λ_i on occupations c_j and on effective interactions $v_{ij} = (V_{ij}^{AA} - 2V_{ij}^{AB} + V_{ij}^{BB})$ are determined by Eq. (5). Generalized mobility $M_{ij}(c_k)$ for DAE models has the following general form:

$$M_{ij} = \gamma_{ij}^{AB} B_{ij} \exp\left[\beta(\lambda_i + \lambda_j)/2\right]; \qquad B_{ij} = \langle n_i' n_j' \exp\left[\beta \sum_{l \neq i,j} (u_{il} + u_{jl}) n_l\right]\rangle \tag{6}$$

where $n_i' = (1 - n_i)$, and "kinetic potentials" u_{ij} are $(V_{ij}^{AB} - V_{ij}^{BB})$. For VME models, the appropriate "effective mobilities" in (4) will be shown to have the form similar to Eq. (6).

To find functions $\lambda_i\{c_j\}$ and $M_{ij}(c_k)$ from Eqs. (5) and (6), we should use some method of statistical calculations, such as kinetic mean-field approximation (KMFA), or kinetic pair cluster approximation (KPCA). At low concentrations and temperatures c, T under consideration, KMFA can not be used as it yields order-of magnitude errors for all main parameters of processes, such as the supersaturation s. On the contrary, KPCA at low c and T is, generally, highly accurate, and below we use only KPCA.

For further generalizations, we also rewrite QKE (4) in the "finite difference" form, integrating it over a small time interval δt:

$$\delta c_i = \sum_j M_{ij}\, 2\sinh[\beta(\lambda_j - \lambda_i)/2]\delta t. \qquad (7)$$

Now we note that the QKE (4) or (7) determine evolution of concentrations c_i due to the averaged atomic fluxes, and they can be shown to describe only those processes in which the total free energy F_{tot} decreases. However, nucleation processes should be accompanied by a local increase of F_{tot} to overcome nucleation barriers, and to describe it we should also consider the fluctuations of atomic fluxes. To this end we first note that the GGD approach, being a statistical description based on "ensemble averages" $c_i = \langle n_i \rangle$, is physically informative and complete only for those non-equilibrium systems which can be divided into some locally equilibrated subsystems (called in textbooks "quasi-closed subsystems") for which the site chemical potential λ_i is approximately constant, with the size $l_{\rm le}$ much exceeding the interatomic distance. Thus summation over alloy states in Eq. (5) should include the distributions $\{n_i\}$ with only not too large inhomogeneity lengths $l < l_{\rm le}$, while long-wave fluctuations with $l \gtrsim l_{\rm le}$ are fixed in the non-equilibrium state under consideration. Therefore, the "diffusive" term entering QKE (7) corresponds to the averaging only over the short-ranged fluctuations at the fixed long-wave fluctuations, and the terms describing the dynamics of these long-wave fluctuations should also be considered.

Stochastic kinetic equation

To describe these fluctuative terms, we use the stochastic approach of the type suggested by Langevin for mechanical systems, proceeding from averages $\langle n_i \rangle = c_i$ to the "individual phase trajectories", that is, to fluctuating occupation numbers $n_i(t)$ averaged only over the quasi-closed subsystem to which it belongs. It differs from the full average $\langle n_i \rangle$ due to the long-wave fluctuations of atomic transfers δn_{ij}^f across each bond ij (that connects the site i with some its neighbor j) for the time interval δt. Thus instead of the QKE (7) we obtain the stochastic kinetic equation (SKE):

$$\delta n_i \equiv n_i(t+\delta t) - n_i(t) = \delta n_{di}\{c_j\} + \sum_j \delta n_{ij}^f \tag{8}$$

where the diffusive term δn_{di} means the right-hand side of the QKE (7). Then we treat each fluctuative transfer δn_{ij}^f as a random quantity with the Gaussian probability distribution:

$$W(\delta n_{ij}^f) = A_{ij} \exp[-(\delta n_{ij}^f)^2 / 2 D_{ij}] \tag{9}$$

where A_{ij} is the normalization constant, and the dispersion D_{ij} is the same as that for the actual fluctuative transfer δn_{ij}^f. For small time intervals $\delta t \ll 1/M_{ij}$, the dispersion D_{ij} is simply related to the mobility M_{ij}:

$$D_{ij} = \langle (\delta n_{ij}^f)^2 \rangle = 2 M_{ij} \delta t. \tag{10}$$

Filtration of noises

Unlike standard applications of the Langevin-noise method to mechanical systems, for statistical systems under consideration it should be supplemented by the "filtration of noise" procedure which eliminates short-wave contributions to the fluctuations δn_{ij}^f (these contributions are actually included into the diffusive term δn_i^d of Eq. (4) obtained by statistical averaging over these short-wave fluctuations). Thus, in the last term of SKE (8), the full fluctuative transfer δn_{ij}^f should be replaced by its long-wave (or "coarse-grained") part δn_{ij}^{fc}. The latter is obtained by introducing a proper cut-off factor $F_c(\mathbf{k})$ in the Fourier-component $\delta n_{f\alpha}(\mathbf{k})$ of the full function $\delta n_{ij}^f \equiv \delta n_\alpha^f(\mathbf{R}_{s\alpha})$ where $\mathbf{R}_{s\alpha}$ denotes the position of the center of bond ij in the appropriate sublattice α formed by these bond centers in the crystal:

$$\delta n_{f\alpha}^c(\mathbf{R}_{s\alpha}) = \sum_{\mathbf{k}} \exp(-i\mathbf{k}\mathbf{R}_{s\alpha})\, \delta n_{f\alpha}(\mathbf{k})\, F_c(\mathbf{k}); \qquad \delta n_{f\alpha}(\mathbf{k}) = \frac{1}{N}\sum_{\mathbf{R}_{s\alpha}} \exp(i\mathbf{k}\mathbf{R}_{s\alpha})\, \delta n_{f\alpha}(\mathbf{R}_{s\alpha}). \qquad (11)$$

The cut-off factor $F_c(\mathbf{k})$ can be taken in the following simplest form:

$$F_c(\mathbf{k}) = \exp\left[-g^2 \sum_{nn} (1 - \cos \mathbf{k}\mathbf{R}_{nn})\right], \qquad (12)$$

where $\mathbf{R}_{nn}$ are the nearest-neighbor lattice vectors in the crystal lattice considered. For the large $g^2 \gg 1$ used, the cut-off factor $F_c(\mathbf{k})$ is reduced to the gaussian $\exp(-k^2 l^2/2)$ with $l_c = ga$ where a is the lattice constant. Thus, quantity $l = ga$ has the meaning of a characteristic size l_{le} of the locally equilibrated regions (quasi-closed subsystems) mentioned above.

Equivalence of precipitation kinetics for the vacancy exchange models to that for certain direct exchange models

Vacancy concentration c_{vi} is quite small. Therefore, the relaxation times for distributions of atoms A in an ABv alloy are by factor $1/c_{vi}$ larger than the time of the relaxation of vacancies at the given distribution of c_{Ai} to their equilibrium distribtion $c_{vi}\{c_{Ai}\}$. The resulting "adiabaticity equation" $dc_{vi}/dt = 0$ can usually be solved either exactly or approximately. It yields:

$$\gamma_{\mathrm{AB}}^{eff} = \gamma_{\mathrm{vA}}\gamma_{\mathrm{vB}}\nu(t), \qquad t_r = \int_0^t \gamma_{\mathrm{AB}}^{\mathrm{eff}}(t')dt'$$

where $\nu(t)$ is some "spatially self-averaged" function of concentrations c_{vi} and c_{Ai}.

Vacancy trapping and "equivalence theorem" for the Belashchenko and Vaks (1998) model

c_{Ai}

c_{vi}

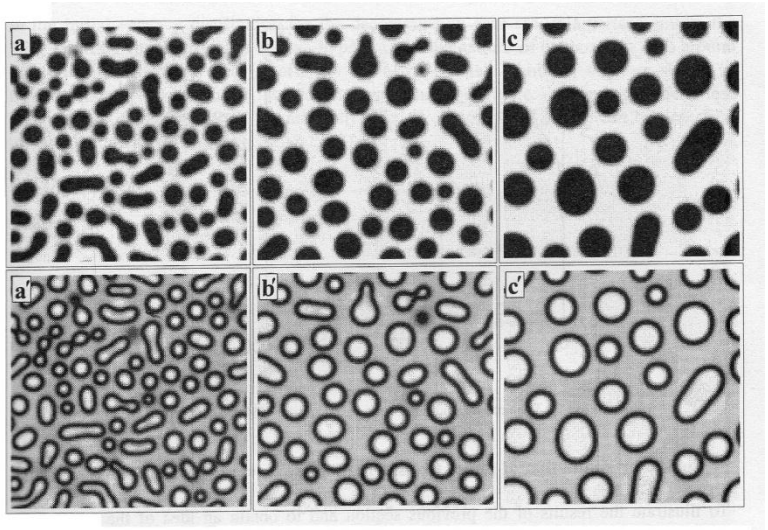

c_{Ai}

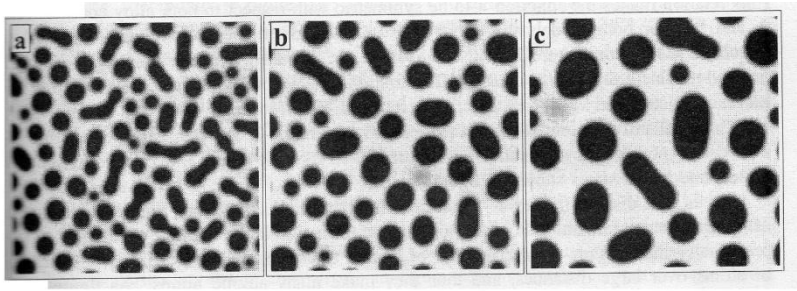

Rescaling of time

SF model at T = 773 K and c = 1.34 at.

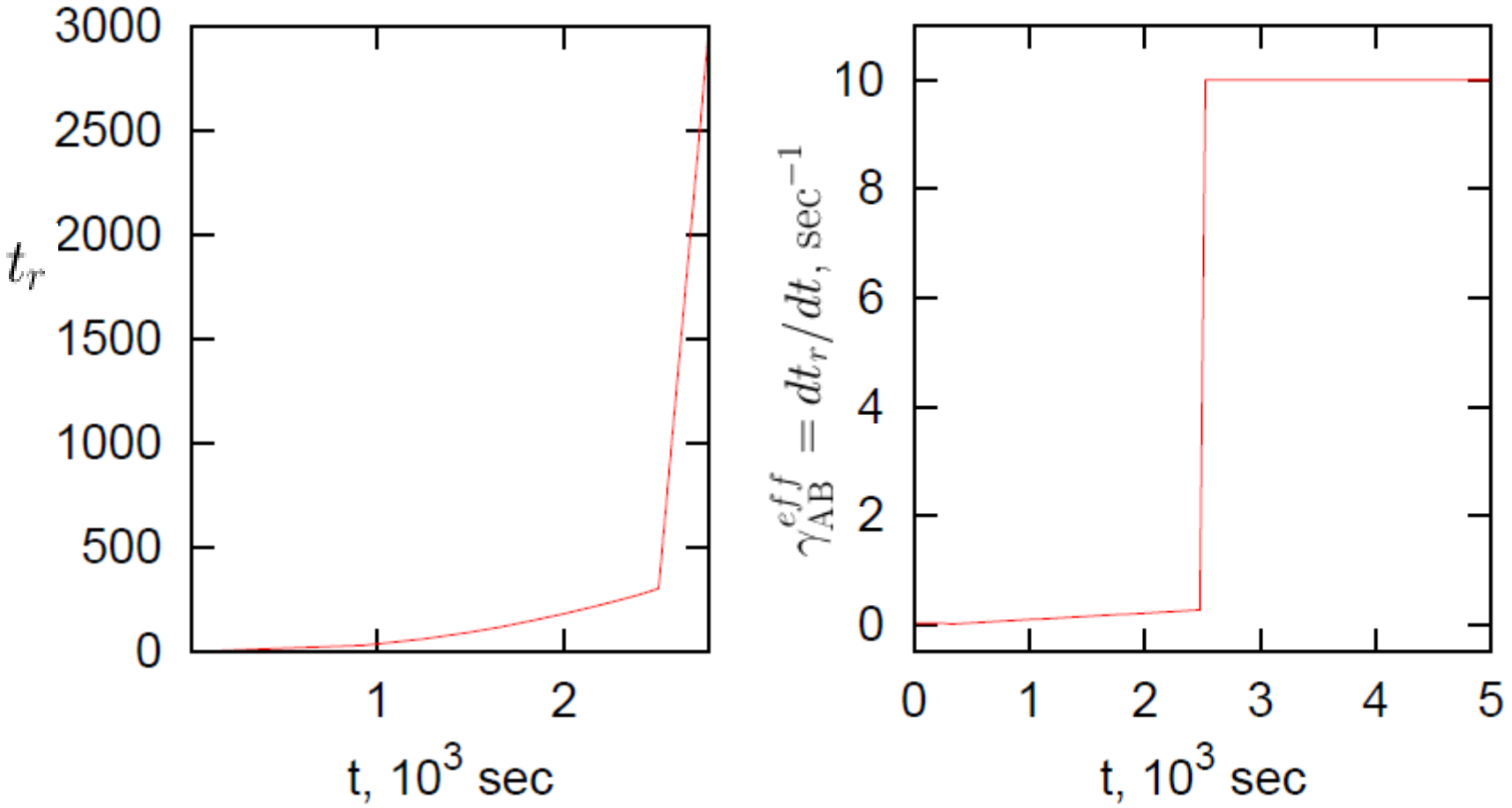

Left: Dependence of reduced time t_r (of the mean number of inter-site exchanges A↔B per site) on physical time t for the SF-1 model found from comparison of the SSA and KMCA simulation results. Right: Same for the effective A↔B exchange rate $\gamma_{\rm AB}^{eff} = dt_r/dt$.

Alloy models used for simulations

Soisson and Fu, 2007 (SF)

Le Bouar and Soisson, 2002 (LBS)

Interactions (in K)

$v_1 = -1400 + 0.18T$, $v_2 = -240 + 0.09T$,
$u_1 = -1470 - 0.09T$, $u_2 = 510 - 0.05T$

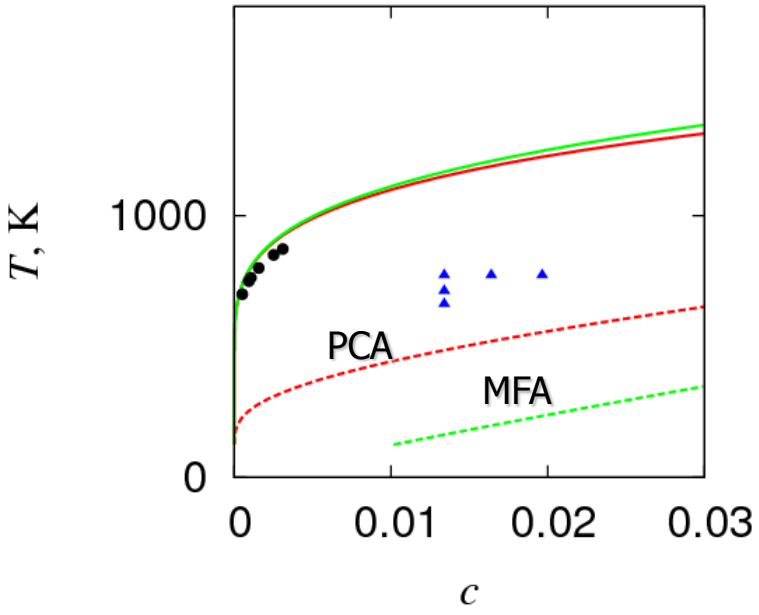

$v_1 = -2300$, $u_1 = 1800$

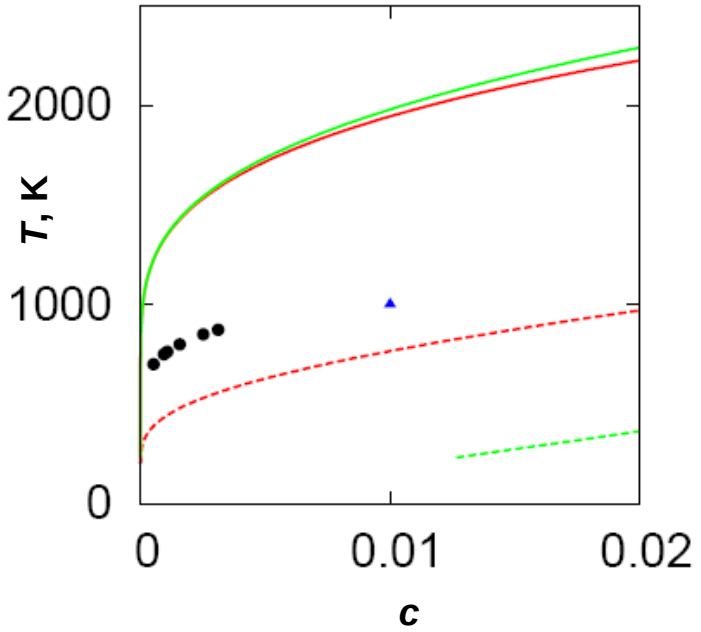

Solid lines – binodals, dashed lines – spinodals. Red lines – pair cluster approximation (PCA), green lines – mean-field approximation (MFA), black circles – CALPHAD estimated binodals, triangles – points used for simulations

Soisson and Martin (2000)

This work appears to be the first microscopic study of the decomposition kinetics in metastable alloys made using detailed kinetic Monte Carlo simulations for some simple alloy model. As the nucleation barrier and the critical embryo size for this model are rather large, the classical theory of nucleation here is expected to be adequate, and it was basically demonstrated in this work.

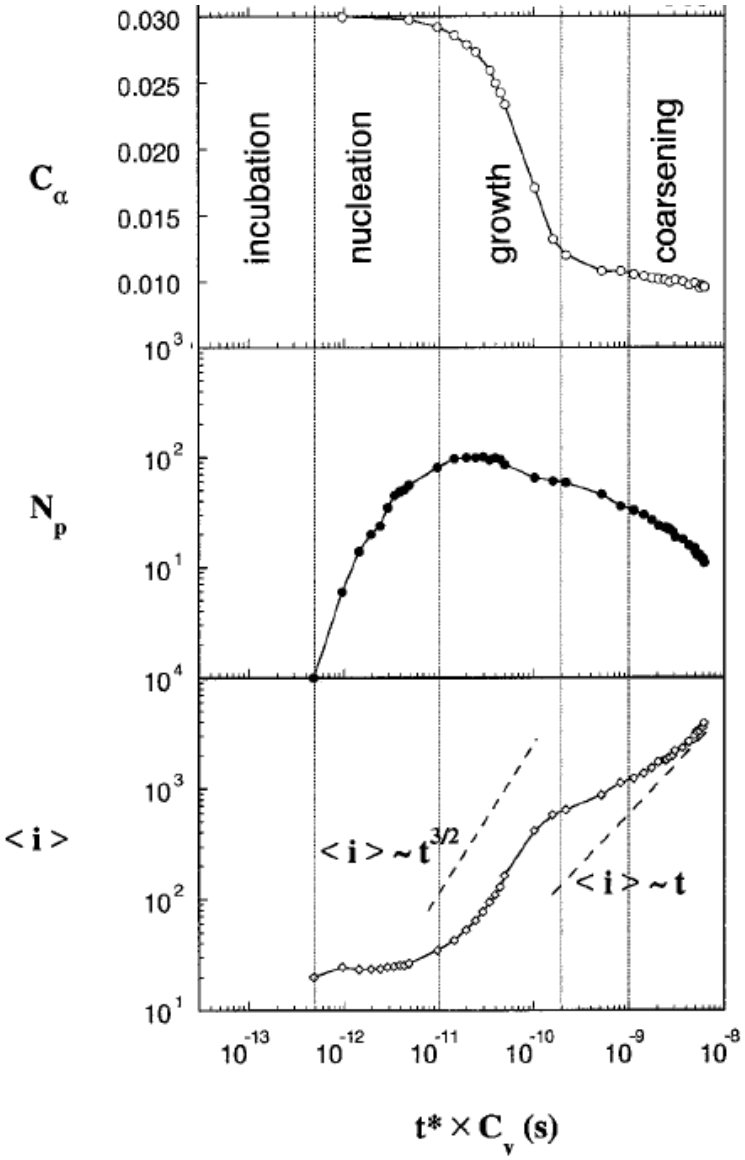

Concentration profiles and parameters of thermodynamic critical embryos found using Dobretsov and Vaks (1998) method

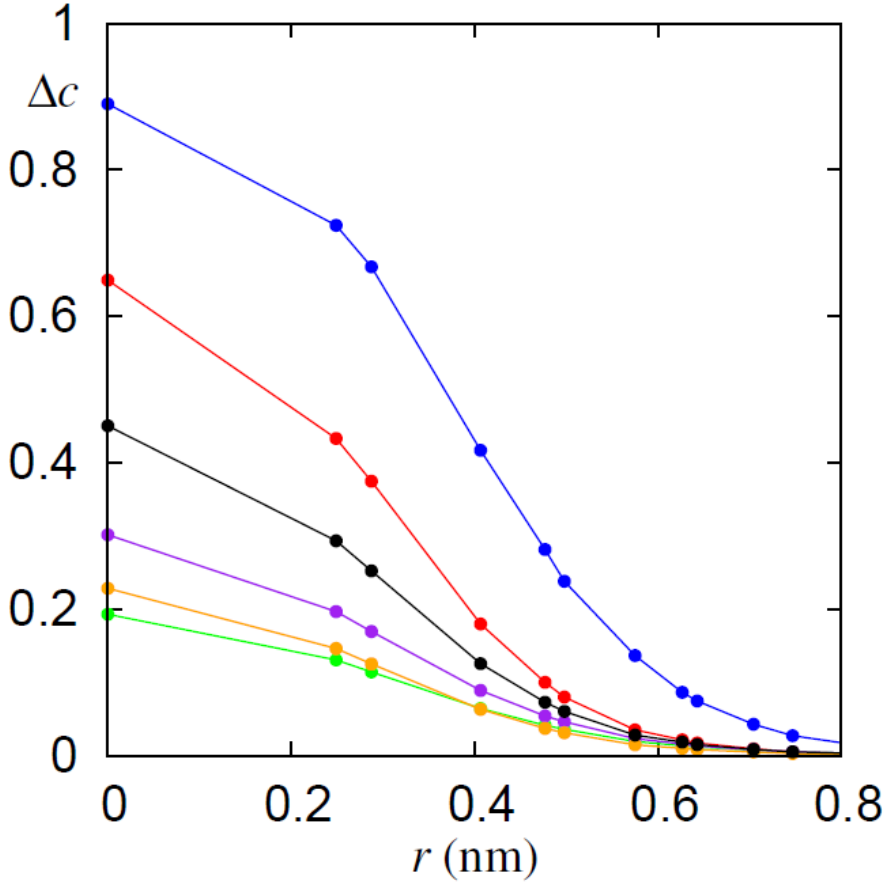

Supersaturation, nucleation barrier F_c and the number of atoms in critical embryo N_c

Alloy state	s	F_c/T	N_c
Soisson and Martin, 2000 (blue)	0.29	7.48	33.8
SF, T = 773 K (SF-1) c=1.34 % (red)	0.29	4.38	14.3
SF, T = 713 K (SF-2) c=1.34 % (black)	0.35	2.47	10.7
SF, T = 663 K (SF-3) c= 1.34 % (purple)	0.43	1.36	8.2
LBS , T= 1000 K, c=1 % (green)	0.46	0.83	6.2
SF, T = 561 K, c=0.078% (orange)	0.39	1.1	5.0

Estimating the local equilibrium length $l = ga$ from the "maximum thermodynamic gain" principle

As mentioned, the reduced length $l = ga$ in our equations characterizes sizes of locally equilibrium quasi-closed subsystems used in the statistical description of a nonequilibrium alloy. The actual distribution of these lengths in an alloy varies with both space and time; in particular, after creation of a supercritical precipitate, the degree of local equilibrium in the adjacent region should significantly increase with respect to other regions where such precipitates are not born yet.

For simplicity we characterize the distribution of all local lengths $l(\mathbf{r})$ by a single spatially averaged parameter $l = ga$ where the reduced length $g = l/a$, generally, varies with the evolution time t or reduced time t_r. After completion of nucleation at some $t_r = t_N$, the alloy rapidly approaches the full two-phase equilibrium. Thus the length $l(t_r) = ga$ at $t_r \gtrsim t_N$ should become large, fluctuative terms in our stochastic equations become small, and the SKE transforms into the QKE with no fluctuation terms.

To describe the above-discussed physical picture with the minimal number of model parameters, we approximate the time dependence $g(t_r)$ by the following simple expression:

$$g(t_r) = g_0(1 + t_r^2/t_0^2), \tag{1}$$

which includes two parameters to be determined: g_0 expected to be of the order of reduced size of critical precipitates: $g_0 \sim R_c/a$, and t_0 of the order of reduced nucleation time t_N.

Estimating the local equilibrium length $l = ga$ from the "maximum thermodynamic gain" principle

To estimate g_0 and t_0, we try to extend the second law of thermodynamics, that is, the principle of minimum of free energy with respect to all its free parameters (valid for equilibrium systems) to the kinetics of non-equilibrium systems studied. To this end we note that main characteristics of microstructure formed in the course of the nucleation process, including the characteristic local equilibrium length l or the length of local non-uniformity of chemical potentials $l_{nu} \sim l$, can be treated as "free" parameters of structure of a nonuniform nonequilibrium state analogous to "static" free parameters in equilibrium systems. Thus it seems natural to suggest that the kinetic path of evolution of this nonequilibrium state should correspond to the maximum thermodynamic gain, that is, to the maximum rate of decrease of free energy. This suggestion can extend the "excess entropy production" approach to thermodynamics of irreversible processes discussed by Prigogine for open systems to the closed non-equilibrium systems under consideration. Then parameters g_0 and t_0 can be estimated from the condition of maximum thermodynamic gain in the course of the nucleation process, that is, from minimization of the free energy $F(g_0, t_r)$ at $t_r \sim t_N$ with respect to g_0 and t_0. This free energy is easily calculated by the GGDA methods.

Temporal evolution of the free energy $F(t_r)$ per copper atom and of the total number $N_p(t_r)$ of supercritical precipitates for the Fe-1.5%Cu alloy at 873 K

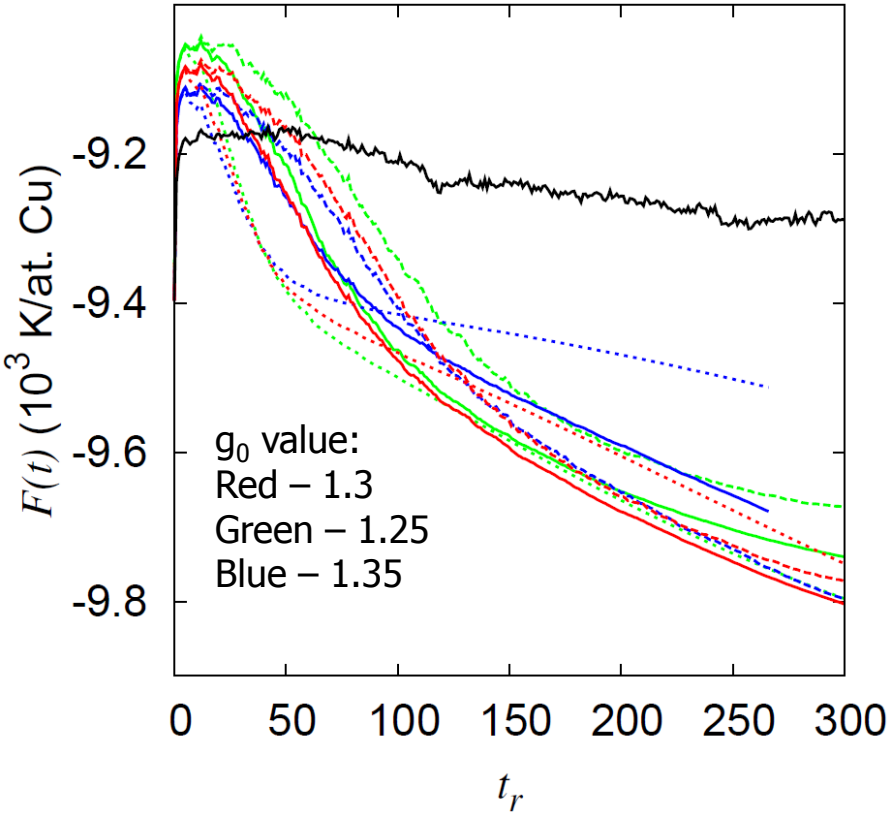

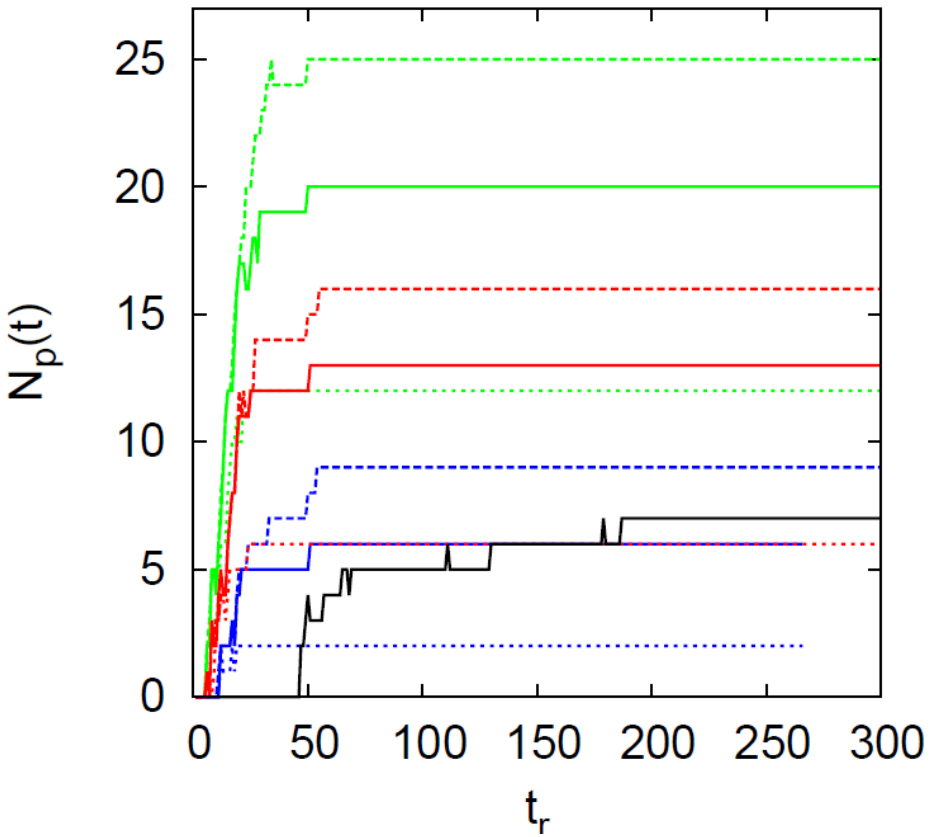

Left: Free energy $F(t_r)$. Right: total number $N_p(t_r)$ of supercritical precipitates (those which contain $p \geq p_c = 21$ copper atoms) within simulation box. Dashed curves: $t_0 = 150$; solid curves: $t_0 = 100$; dotted curves: $t_0 = 50$. Black curves correspond to some more crude, one-parametric model for $g(t)$ with sharp switching off fluctuations at $t > t_N$.

Temporal evolution of the free energy F(t) per copper atom and the total number $N_p(t)$ of supercritical precipitates for the SF-1 model

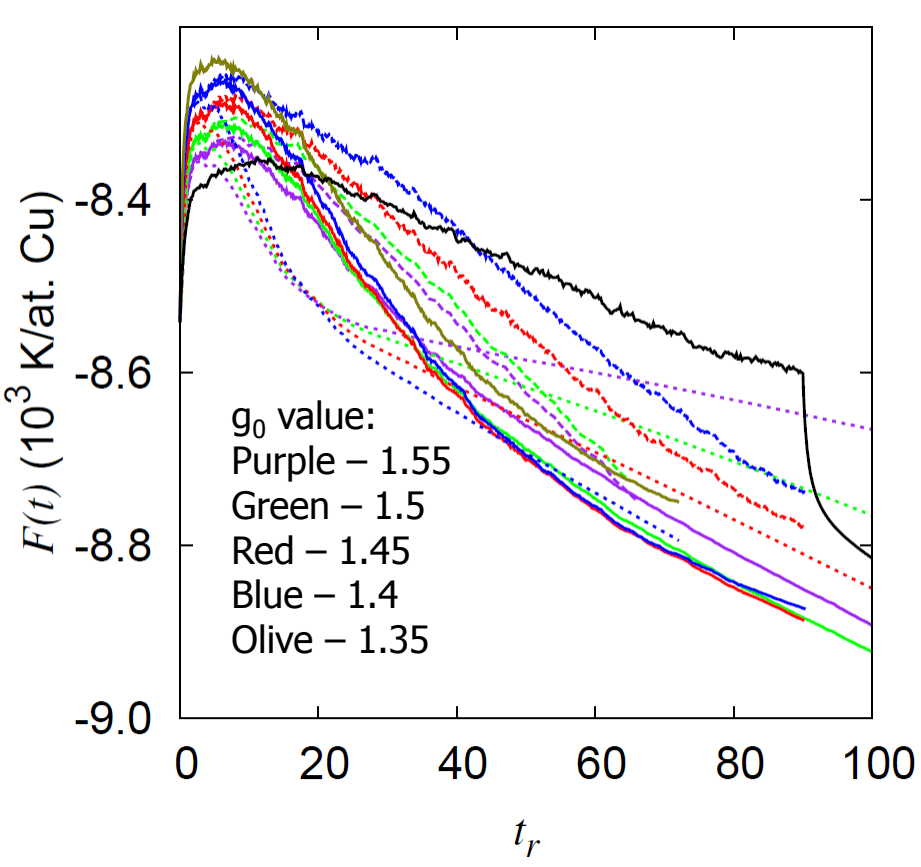

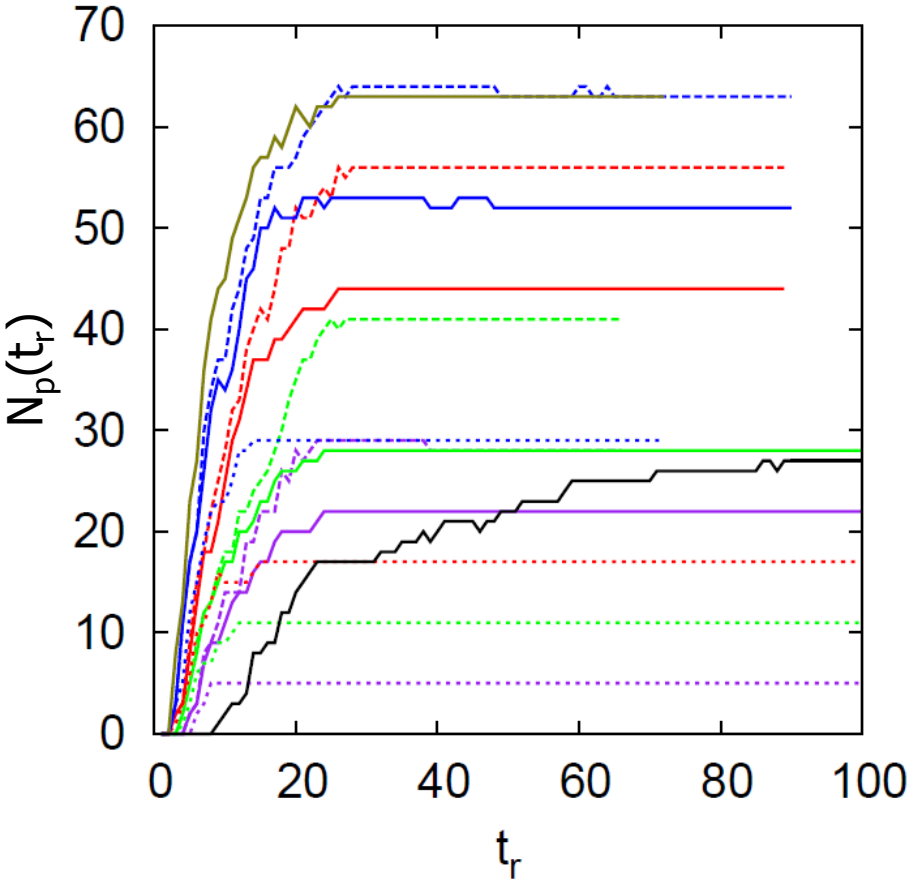

Left figure: Free energy $F(t_r)$. Right figure: total number $N_p(t_r)$ of supercritical precipitates (those which contain $p \geq p_c = 15$ copper atoms) within simulation box. Dashed curves: $t_0 = 100$; solid curves: $t_0 = 50$; dotted curves: $t_0 = 20$.

Comparison of some results of SSA and KMCA simulations For the SF-1 model

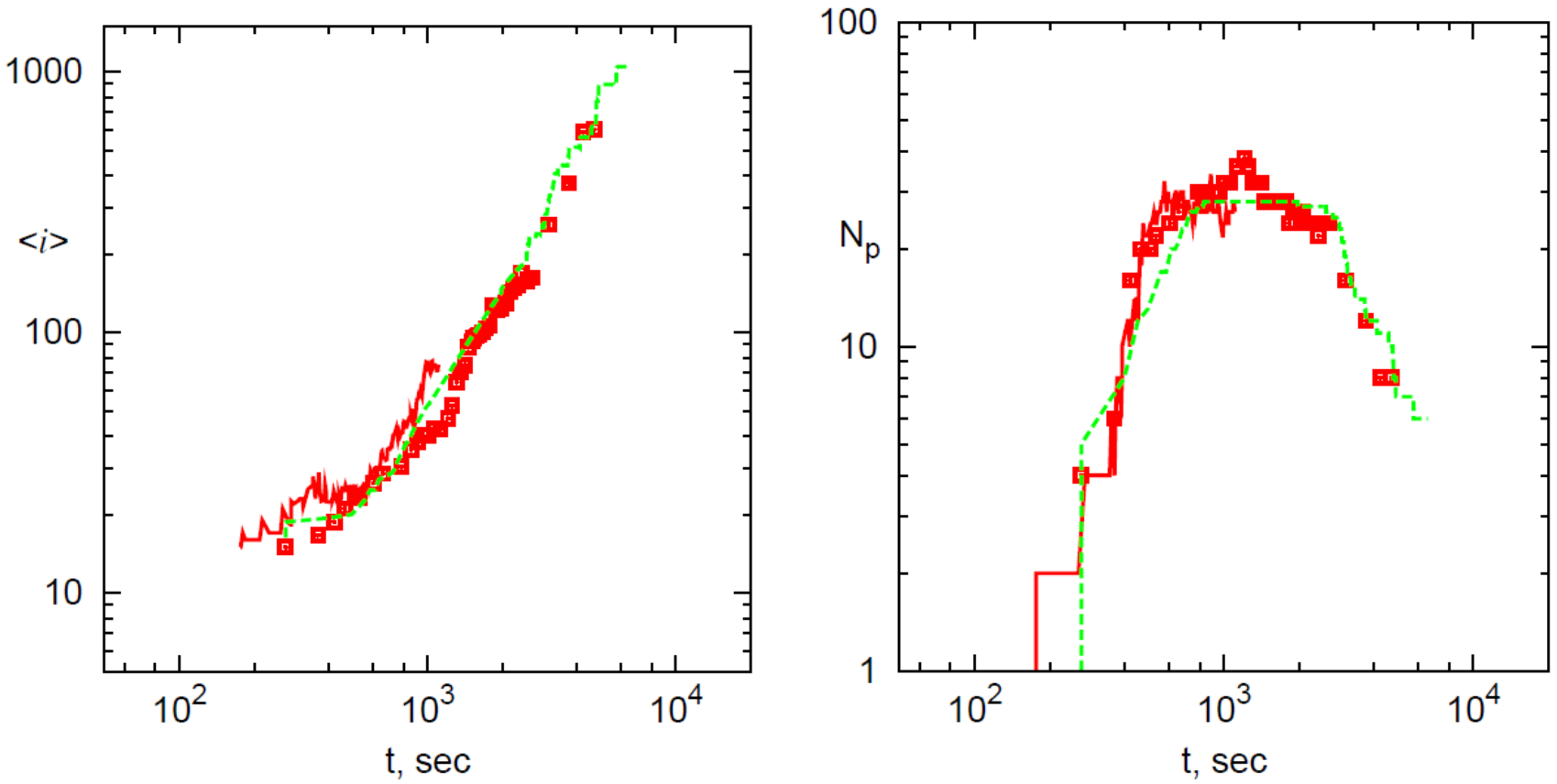

Left: Total number $N_p(t)$ of supercritical precipitates within simulation box. Right: Average number of atoms within a precipitate ("average precipitate size") $\langle i(t) \rangle$. Red curves or squares show the results of two different KMCA runs. Green dashed curves show the SSA results.

Kinetics of very first stages of nucleation for SF-1 model

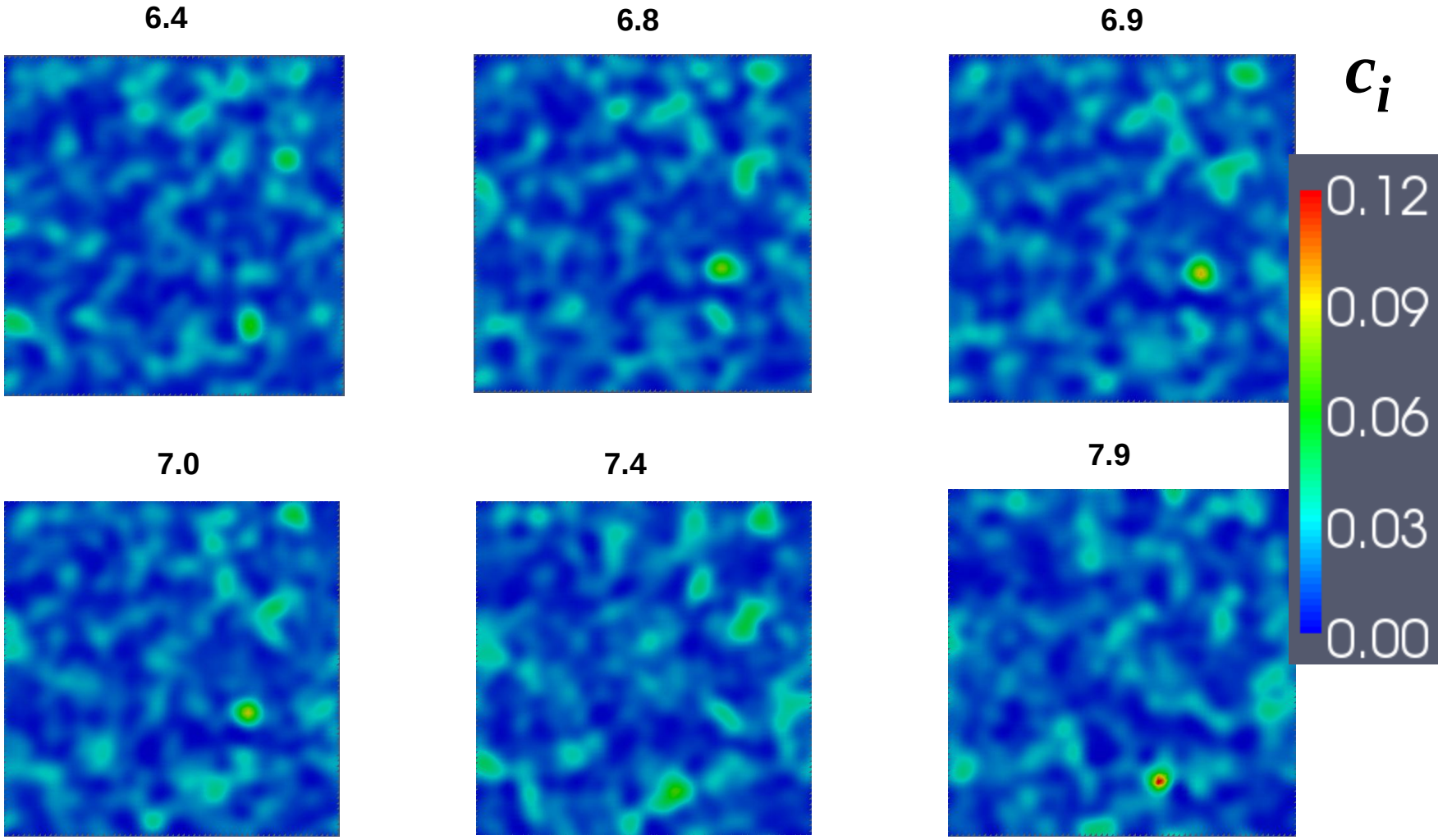

Evolution of concentration within a plane containing several nucleating precipitates observed in SSA simulation for the SF-1 model at the reduced time t_r values shown near each frame

Kinetics of very first stages of nucleation

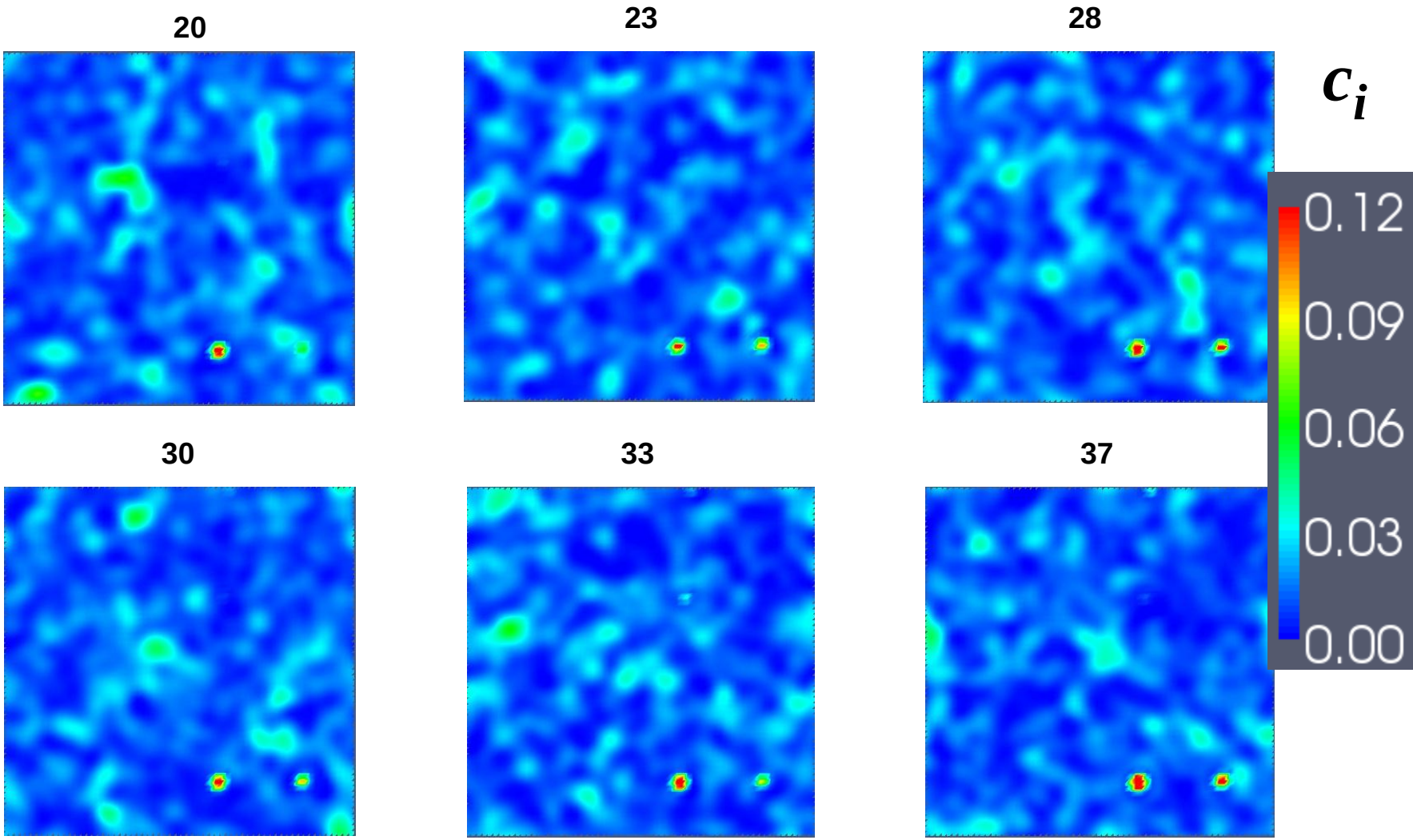

Evolution of concentration within a plane containing several nucleating precipitates observed in SSA simulation for the SF-1 model at the reduced time t_r values shown near each frame

Kinetics of very first stages of nucleation

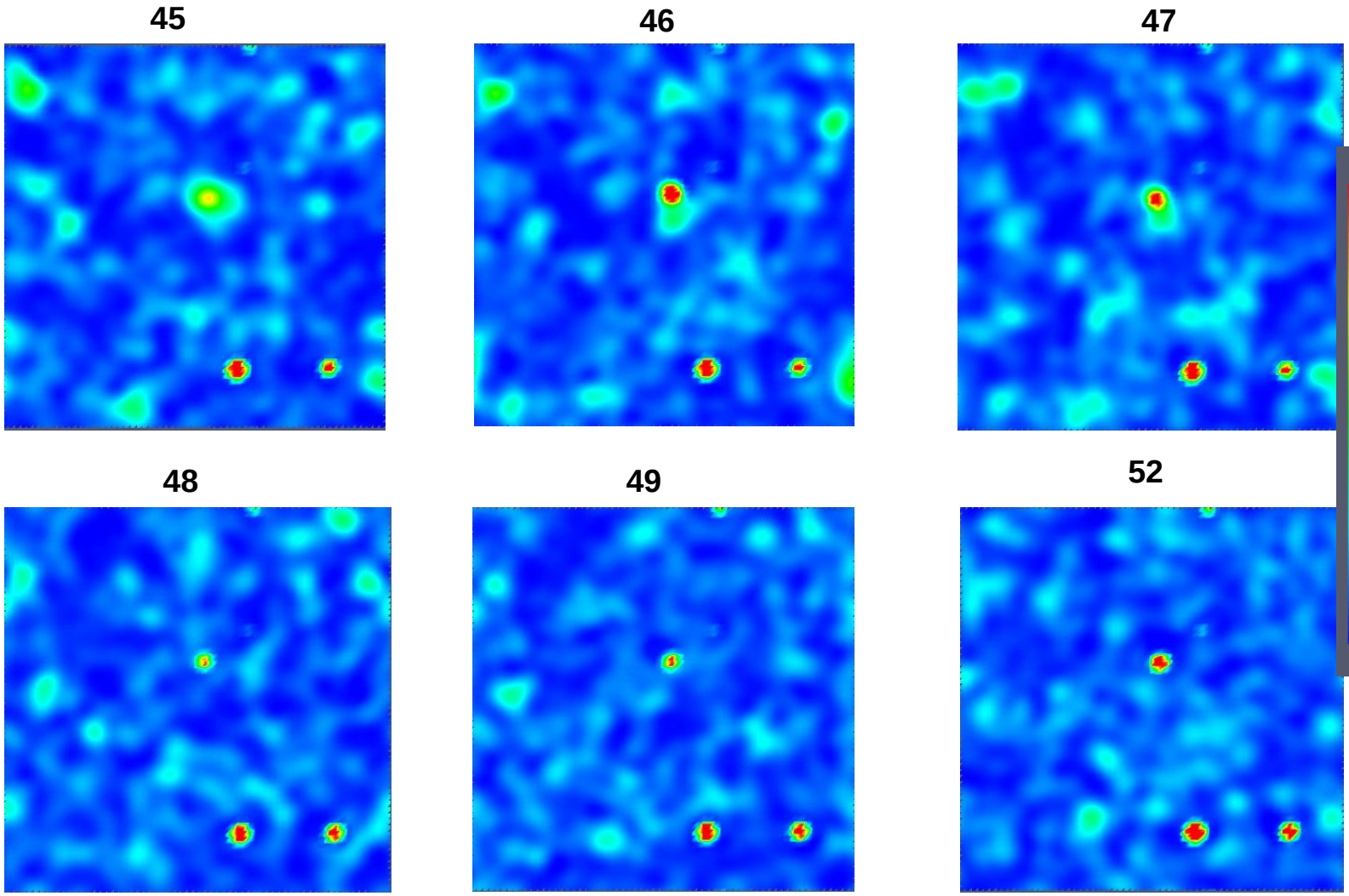

Evolution of concentration within a plane containing several nucleating precipitates observed in SSA simulation for the SF-1 model at the reduced time t_r values shown near each frame

Microstructure at various stages of precipitation

SF-1, T = 773 K, c = 1.34 at %; Simulation volumes $V_s^{SSA} = (64a)^3$; $V_s^{KMCA} = 0.5V_s^{SSA}$

Just before nucleation, t = 55 sec

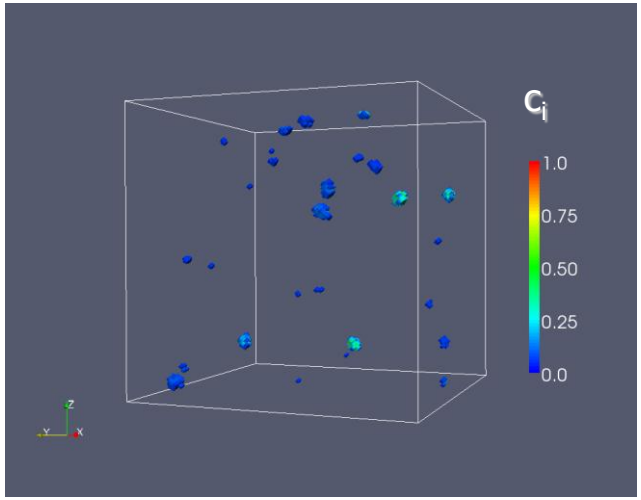

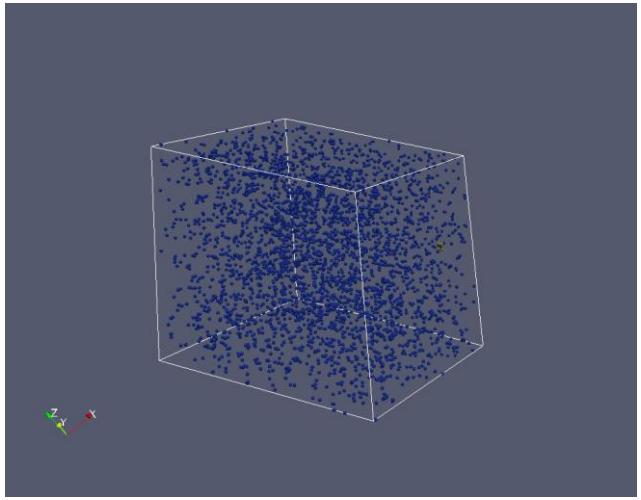

End of nucleation, t = 1000 sec

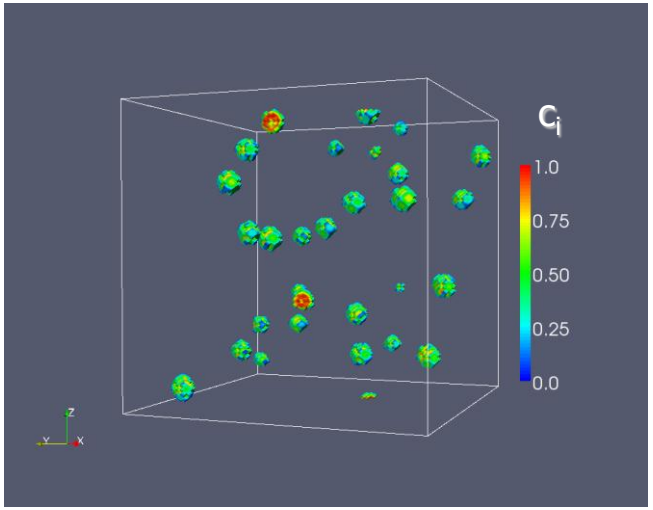

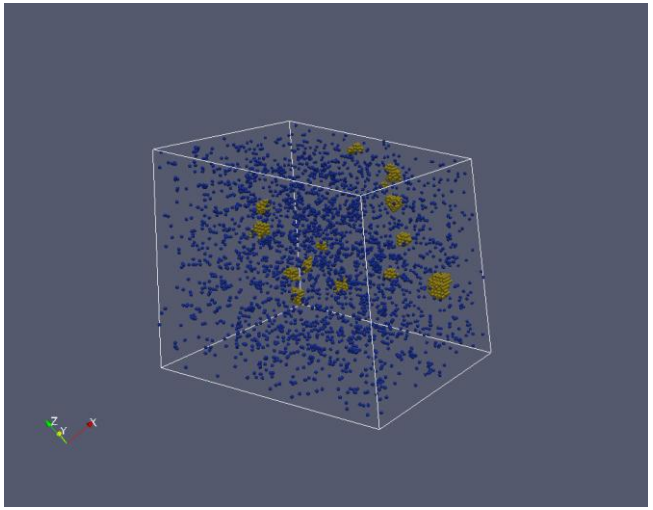

Microstructure at various stages of precipitation

SF, T = 773 K, c = 1.34 at %

Beginning of coarsening, t = 2000 sec

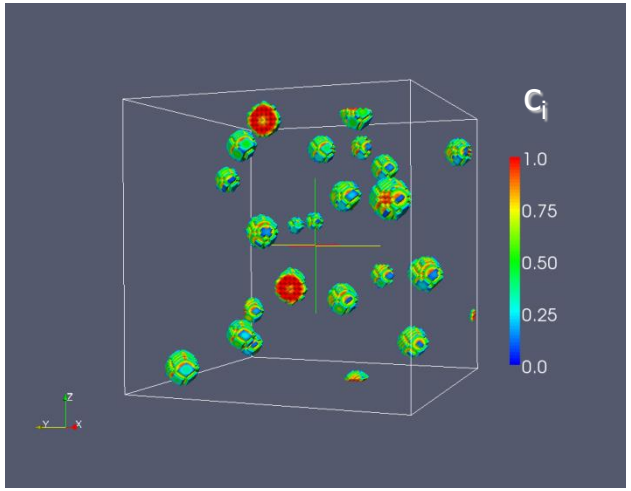

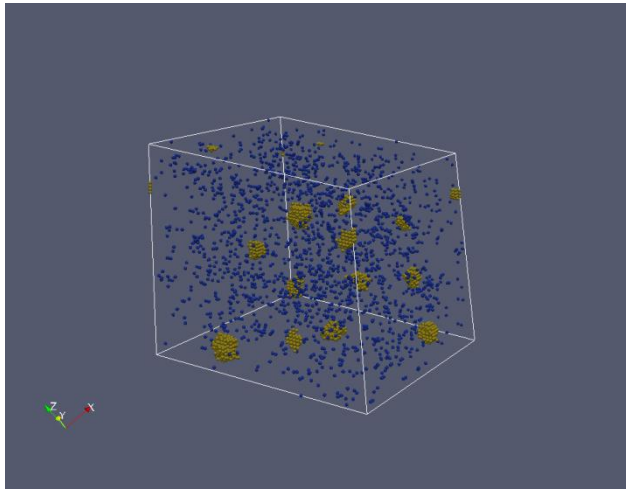

Coarsening, t = 4000 sec

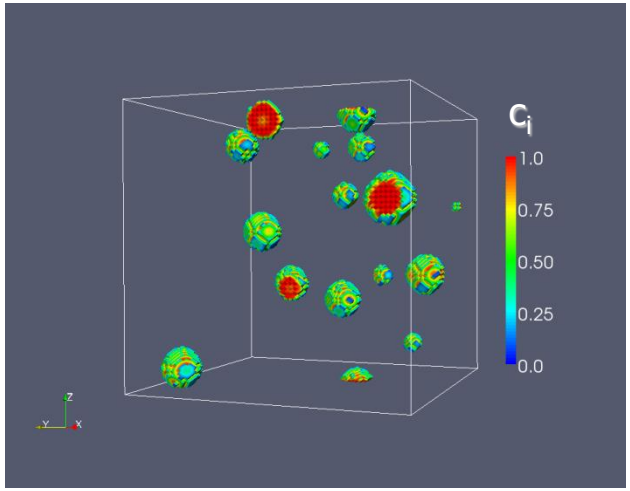

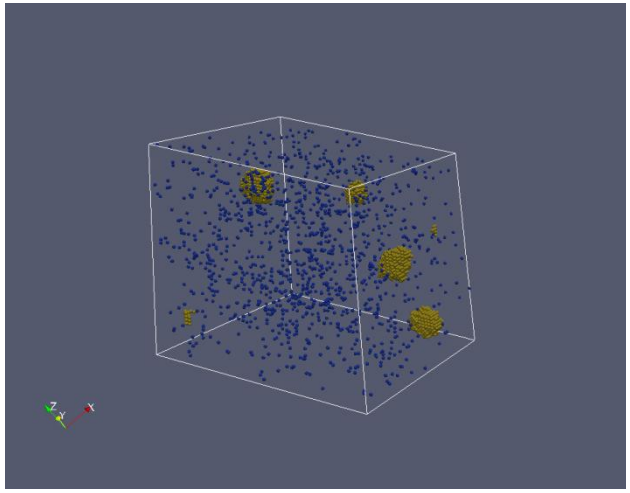

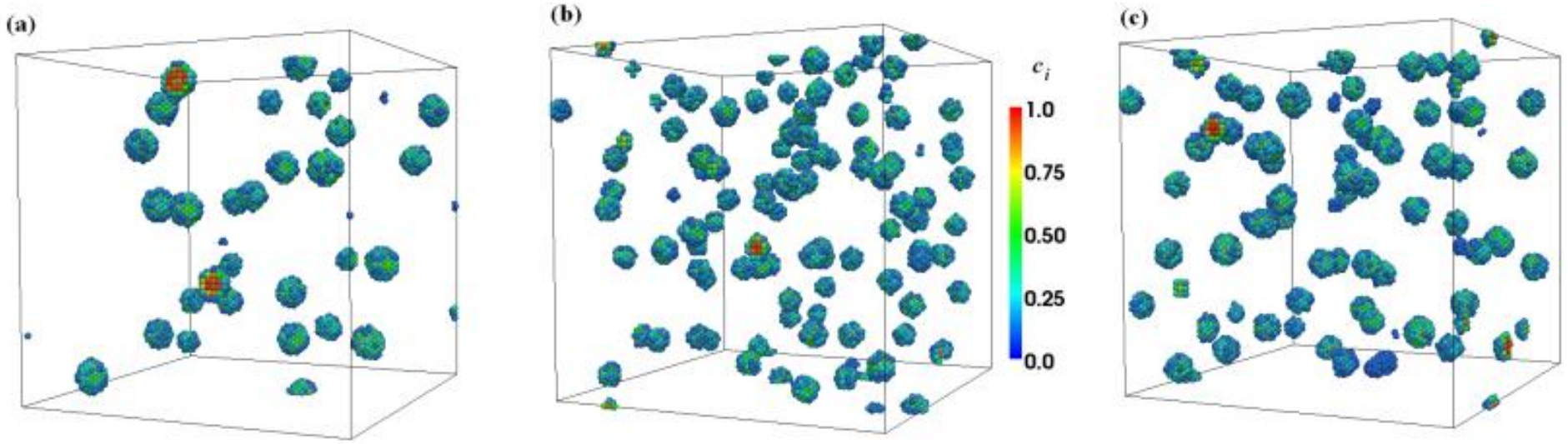

Distribution of concentrations $c_i = c(\mathbf{R}_i)$ at the end of nucleation for the following alloy states:

(a) SF-1, $c = 0.0134$, $T = 773$ K, $s = 0.287$;

(b) SF-3, $c = 0.0134$, $T = 663$ K, $s = 0.425$;

(c) SF-4, $c = 0.0197$, $T = 773$ K, $s = 0.426$.

Precipitation in Ternary Fe-Cu-Mn alloys

In consideration of Fe-Cu-Mn alloys, both configurational interactions v_{ij} and kinetic interactions u_{ij} between Cu and Fe atoms were taken from the SF model described above. Configurational and kinetic interactions of Mn with Fe and Cu have been estimated using the available empirical description of thermodynamics of the Fe-Cu-Mn system (Mittienen, 2003). Our simulations were made for two sets of values of temperature and composition :

I. Those used by Miller et al. (2003) in their experimental studies of decomposition under neutron irradiation of alloys: (A) Fe-Cu, and (B) Fe-Cu-Mn: $T = 561$ K, $c^{\mathrm{A}}_{\mathrm{Cu}} = c^{\mathrm{B}}_{\mathrm{Cu}}$ =0.78 at.%, and $c^{\mathrm{B}}_{\mathrm{Mn}}$ =1.05 at.%.

II. Those corresponding to recent experiments by Shabadi et al. (2010) at $T = 873$ K, $c^{\mathrm{B}}_{\mathrm{Mn}}$ =1 at.%, and several $c^{\mathrm{A}}_{\mathrm{Cu}} = c^{\mathrm{B}}_{\mathrm{Cu}}$ close to 1.08 at.% used by Shabadi et al.

All microstructural characteristics of precipitation in Fe-Cu-Mn alloys were found to be rather sensitive to both configurational and kinetic interactions of Mn with Cu and Fe. Below we present some results for such values of these interactions which seem to be "most realistic" among those tried in our simulations.

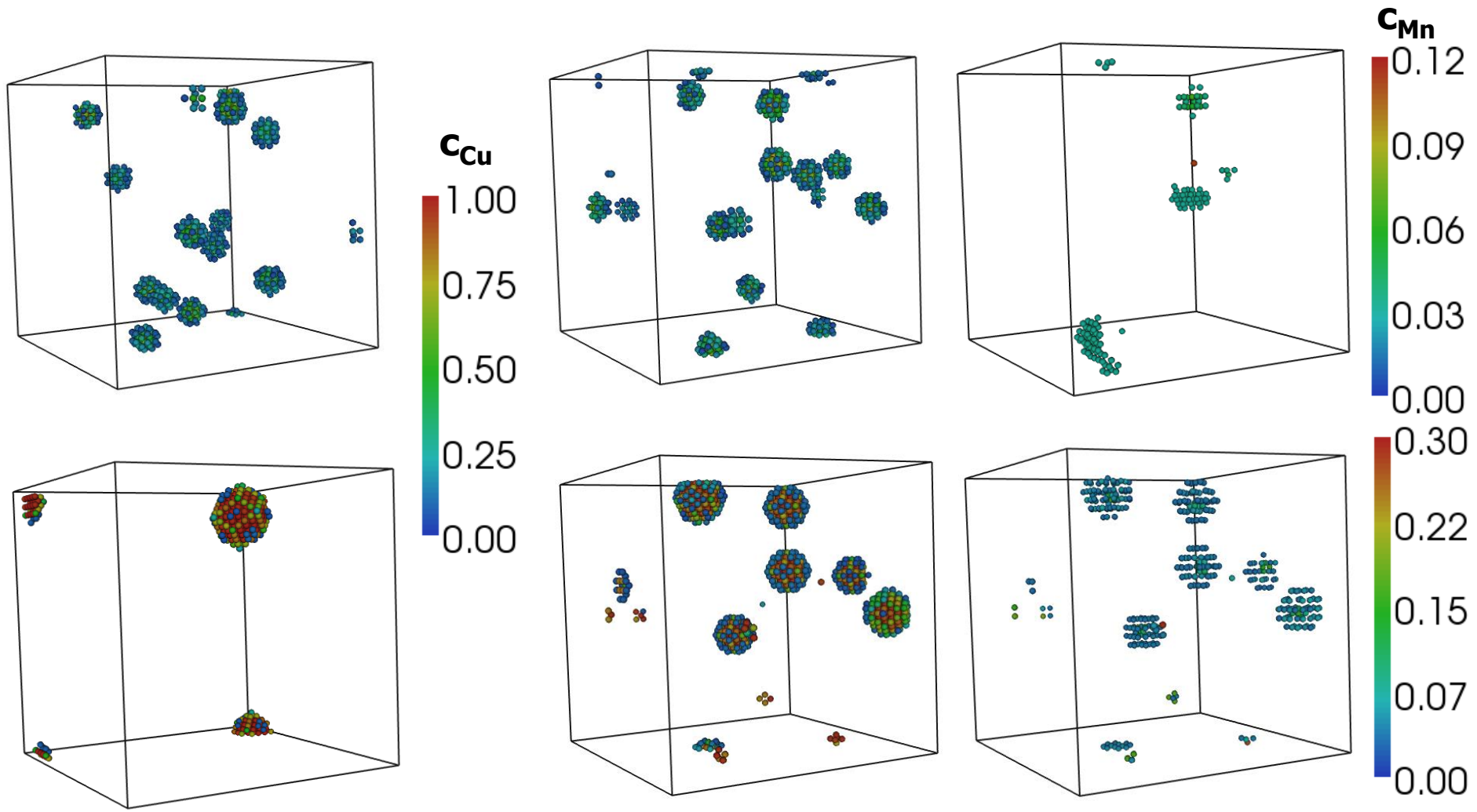

Simulations I. Distribution of local concentrations of Cu and Mn at the end of nucleation (upper row) and at some advanced stage of coarsening (lower row) for the Fe-Cu alloy (left) and for the Fe-Cu-Mn alloy (middle and right), with the following Mn interaction parameters: $v_1^{\mathrm{MnCu}} = -100$ K, $v_1^{\mathrm{MnMn}} = 60$ K, $u_n^{\mathrm{Mn}} = 0$. Only sites i with $c_i^{\mathrm{Cu}} \geq 0.05$ and $c_i^{\mathrm{Mn}} \geq 0.03$ are shown.

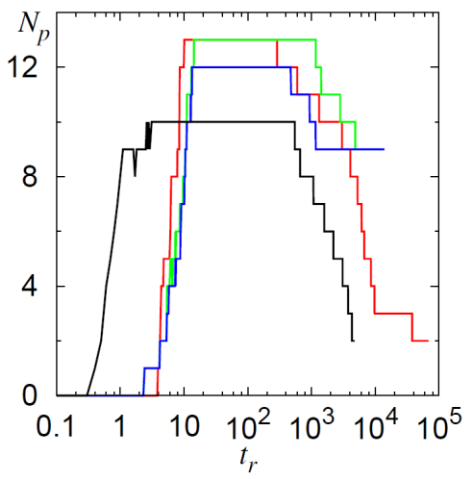

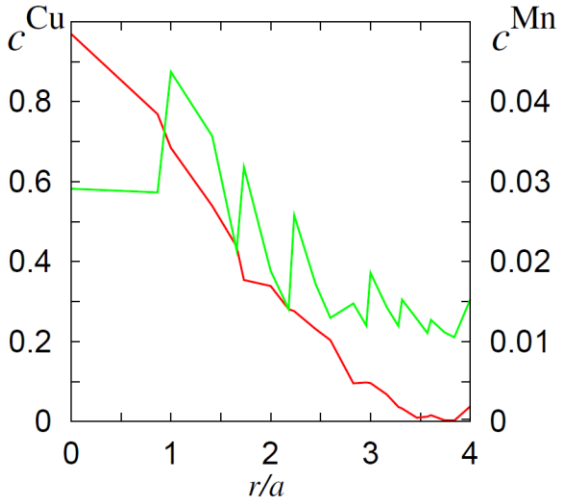

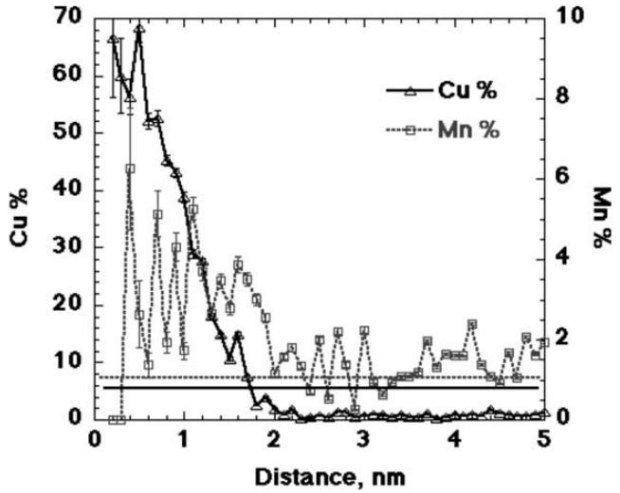

Left: Evolution of total number of supercritical precipitates within simulation box. Red curve corresponds to the simulation for Fe-Cu alloy, the rest curves correspond to the simulations for Fe-Cu-Mn alloy using different kinetic interactions u_n^{Mn} for Mn. Black curve corresponds to some first-principle estimate of u_n^{Mn} (seeming to be unrealistic), while blue and green curves correspond to the estimates of u_n^{Mn} from thermodynamic data. Middle: Concentration profiles averaged over coordination spheres for Cu (red curve) and Mn (green curve) at an advanced stage of coarsening ($t_r = 6000$) observed in the simulation corresponding to the green curve in the left figure. Right: Same as in the middle figure observed in experiments by Miller et al (2003).

Simulations II. Evolution of mean size of precipitates <i(t)> and total number of supercritical precipitates $N_p(t)$ in Fe-Cu and Fe-Cu-Mn alloys at T = 873 K and c_{Cu} = 0.02

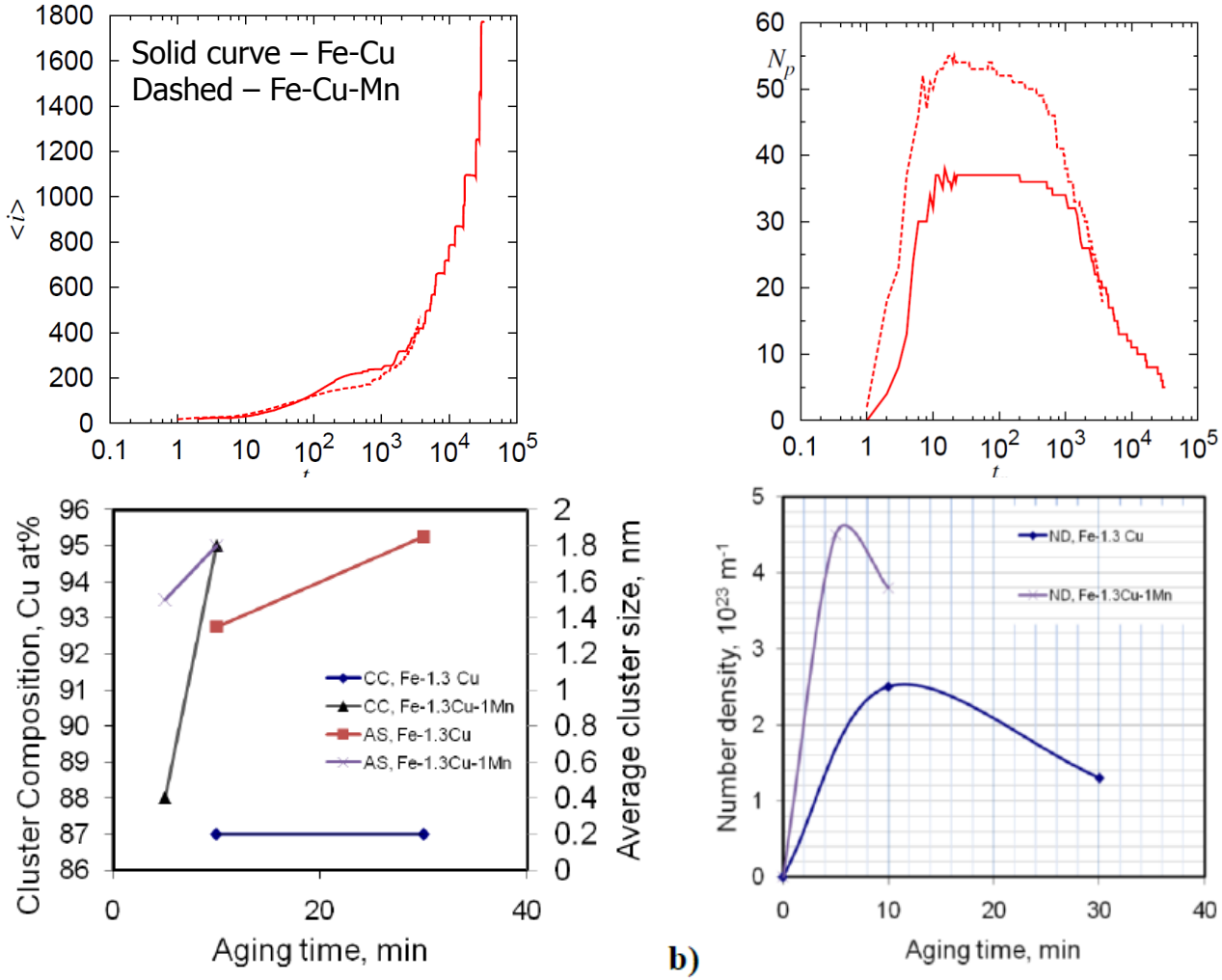

Fig. 3. Evolution of different cluster parameters with the 600°C aging time: a) chemical composition (CC), average size (AS) (radius), b) number density (ND).

Simulations II. Distributions of Cu and Mn atoms at some intermediate stage of coarsening in Fe-Cu-Mn alloys at T = 873 K and c_{Cu} = 2%

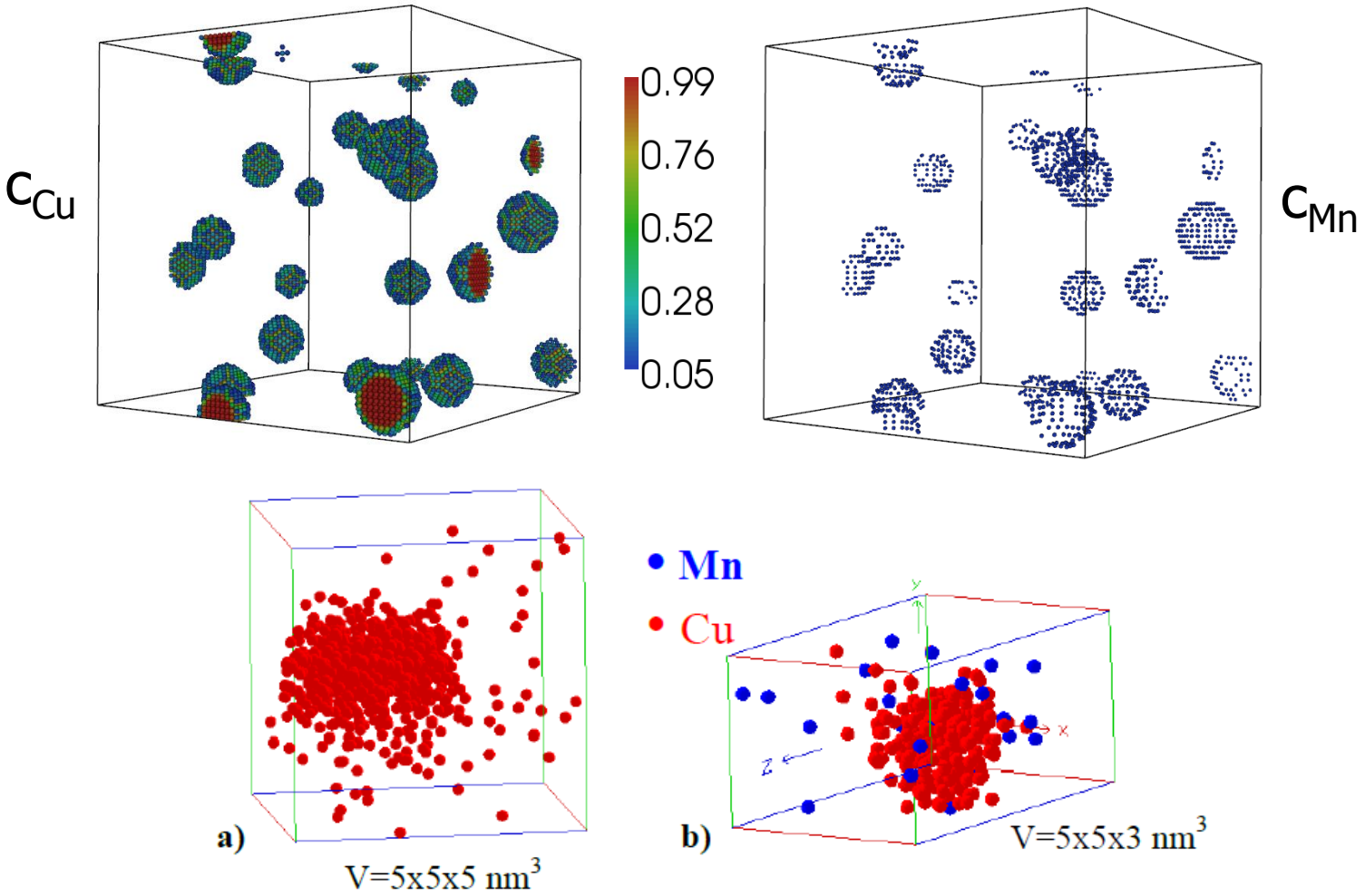

Fig. 2. Individual Cu clusters in the samples aged at 600 °C for 10min: a) Fe-1.3Cu alloy and b) Fe-1.3Cu-1Mn alloy

CONCLUSIONS

1. The consistent and computationally efficient stochastic statistical approach is suggested to study the kinetics of decomposition of metastable alloys.
2. In this approach, description of evolution in terms of certain reduced time includes no adjustable parameters. Rescaling of this reduced time to the physical time can be made with the use of few constants which can be estimated either from comparison to kinetic Monte Carlo simulations or from experiments.
3. For several realistic models of Fe-Cu alloys studied, the results of this approach agree well with the kinetic Monte Carlo results.
4. Application of the methods developed to studies of decomposition of Fe-Cu-Mn alloys revealed a great sensitivity of evolution to the values of both configurational and kinetic interactions between Mn, Cu and Fe atoms. Estimating these interactions from available thermodynamic data, we can well reproduce the main microstructural features of decomposition of Fe-Cu-Mn alloys observed in experiments by Miller et al. (2003) and Shabadi et al (2010).